ACS APPLIED MATERIALS & INTERFACES

Research Article

www.acsami.org

Electrowetting of Nitro-Functionalized Oligoarylene Thiols Self-Assembled on Polycrystalline Gold

Stefano Casalini,*[,†] Marcello Berto,[†] Carlo A. Bortolotti,[†] Giulia Foschi,[†] Alessandra Operamolla,[‡,§] Michele Di Lauro,[†] Omar Hassan Omar,[§] Andrea Liscio,[∥] Luca Pasquali,[⊥] Monica Montecchi,[⊥] Gianluca M. Farinola,[‡,§] and Marco Borsari[#]

[†]Università degli Studi di Modena e Reggio Emilia, Dipartimento di Scienze della Vita, via Campi 183, I-41125 Modena, Italy

[‡]Università degli Studi di Bari "Aldo Moro", Dipartimento di Chimica, via Orabona 4, I-70126 Bari, Italy

[§]Consiglio Nazionale delle Ricerche (CNR), Istituto di Chimica dei Composti Organometallici (ICCOM), via Orabona 4, I-70126 Bari, Italy

[∥]Consiglio Nazionale delle Ricerche (CNR), Istituto per la Sintesi Organica e la Fotoreattività (ISOF), via Gobetti 101, I-40129 Bologna, Italy

[⊥]Università degli Studi di Modena e Reggio Emilia, Dipartimento di Ingegneria "Enzo Ferrari", via P. Vivarelli 10, I-41125 Modena, Italy

[#]Università di Modena e Reggio Emilia, Dipartimento di Scienze Chimiche e Geologiche, via Campi 183, I-41125 Modena, Italy

Supporting Information

ABSTRACT: Four linear terarylene molecules (i) 4-nitro-terphenyl-4″-methanethiol (NTM), (ii) 4-nitro-terphenyl-3″,5″-dimethanethiol (NTD), (iii) ([1,1′;4′,1″] terphenyl-3,5-diyl)methanethiol (TM), and (iv) ([1,1′;4′,1″] terphenyl-3,5-diyl)dimethanethiol (TD) have been synthesized and their self-assembled monolayers (SAMs) have been obtained on polycrystalline gold. NTM and NTD SAMs have been characterized by X-ray photoelectron spectroscopy, Kelvin probe measurements, electrochemistry, and contact angle measurements. The terminal nitro group ($-NO_2$) is irreversibly reduced to hydroxylamine (−NHOH), which can be reversibly turned into nitroso group (−NO). The direct comparison between NTM/NTD and TM/TD SAMs unambiguously shows the crucial influence of the nitro group on electrowetting properties of polycrystalline Au. The higher grade of surface tension related to NHOH has been successfully exploited for basic operations of digital μ-fluidics, such as droplets motion and merging.

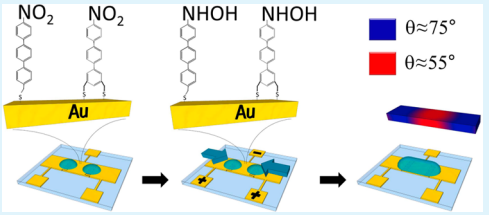

KEYWORDS: *electrowetting on dielectrics, nitro-terminated self-assembled monolayers, conjugated thiols, electrochemistry, micro-electromechanical systems*

INTRODUCTION

Deposition of self-assembled monolayers (SAMs) is a versatile approach to modify metals,[1] organic semiconductors,[2,3] and dielectrics,[4] and it is, in fact, an easy-to-use and low-cost method to tailor chemical−physical features of a substrate of interest.[5] SAMs can be successfully used for several purposes, such as adhesion promotion, corrosion inhibition, lubrication, and wettability,[6] taking advantage of structural diversity of the adsorbing molecules. The molecular scale thickness of SAMs (namely, few nanometers) makes them suitable for fabrication of high-κ dielectrics.[7] For this reason, SAMs were also implemented in organic transistors[8] or in a chip featuring microelectrodes[9] opening toward low-power systems: in fact, their operational voltages were dramatically decreased with respect to comparable systems bearing thicker dielectrics.[7] Since the early 90s, Sondag-Huethorst et al. demonstrated how SAMs can be exploited in the so-called field "electrowetting on dielectrics" (EWOD).[10,11] In particular, it was shown that wettability changed only as consequence of the electrostatic effect arising from the charging of the electrical double layer at dielectric/aqueous solution interface. Electrowetting was also controlled by inducing redox processes at the interface between the dielectric and the liquid phase: in fact, the grafting of an electro-active probe, such as ferrocene, on alkanethiol SAMs formed on a gold substrate showed an enhanced control of electrowetting, which was not governed by charging effects but by the reduction/oxidation of the immobilized redox species.[12]

Electrowetting is based on the modulation of the shape of an air/liquid or liquid/liquid interface by an externally applied electric field.[13] It has been employed in countless technological applications such as adjustable lenses,[14] reflective displays,[15] and microfluidic applications based on droplet actuations.[16]

Among the most interesting developments in the field, the concept of reverse electrowetting (REWOD) is certainly

Received: July 24, 2014
Accepted: February 3, 2015
Published: February 3, 2015

DOI: 10.1021/am509104z
ACS Appl. Mater. Interfaces 2015, 7, 3902−3909

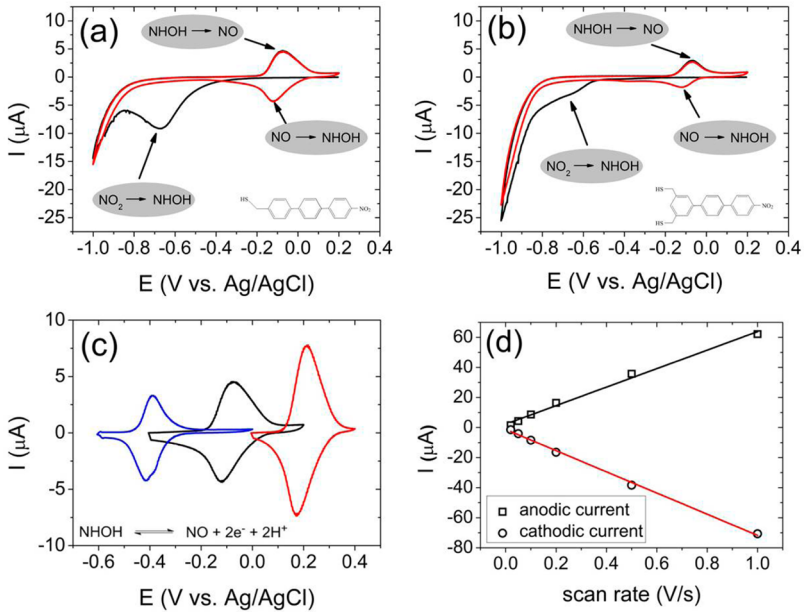

Figure 1. (a) Electro-reduction of NTM-based SAM and (b) NTD-based one at pH 7 (0.1 M KCl buffered by phosphate 10 mM). The first voltammetric cycle is colored in black, and the second one is represented with a red line. (c) Reversible redox signal (NHOH to NO) of NTM SAM at neutral (black line), acid (red line) and basic (blue line) solution. (d) Linear fit of current as a function of scan rate for anodic (black) and cathodic (red) current corresponding to NTM SAM.

worthy of mention.[17] Contrarily to what happens in classical EWOD, which is based on electrical-to-mechanical energy conversion, in REWOD the mechanical energy of the liquid motion onto the dielectric substrate is converted into electrical current. The liquid droplet and an electrode, coated with a dielectric film, are kept at a constant bias voltage by an external electric circuit. Forcing the droplet to move with respect to the electrode generates an excess of surface charge, which causes flow of electrical current in the external circuit.

Recently, droplet jumping by electrowetting (DJE) has also been achieved:[18] the droplets are stretched by asymmetrical electrowetting forces, and when released, the corresponding stored surface energy is converted into kinetic energy for jumping.

Electrowetting can also occur at the interface between two immiscible electrolytic solutions (ITIES): in this case, electrical double layers are formed at the liquid/liquid interface.[13,19,20] This approach can lead to system architectures yielding electrowetting responses at ultra-low potentials (<1 V), thus not requiring the presence of an insulating layer as in EWOD and paving the way for electrowetting devices on conductive substrates.[13]

In the case of SAM-based EWOD, it is possible to adjust and gain further control on the electrowetting phenomena by tailoring the molecular properties of the molecules forming the monolayer. In fact, one can choose between (i) single or multiple anchoring groups,[21] (ii) aliphatic and/or aromatic backbones,[22−24] and (iii) different terminal groups[25,26] (e.g., hydroxyl, carboxyl, nitro, amino etc.). Tuning of the surface tension has been achieved by changing the chemical nature of the functional group facing the solution, switching from a hydrophobic to a hydrophilic one.[27,28]

Within the wide library of electroactive functional groups, $-NO_2$ is one of the most versatile because of its capability to be transformed into different chemical species, which are all pH-dependent.[29] In particular, SAMs from nitro-terminated molecules have been widely employed in organic electronics owing to its dipole moment along with its electron withdrawing capability. In fact, these SAMs have been applied in organic field-effect transistors (OFETs),[30,31] organic light-emitting diodes (OLEDs),[32] and organic photovoltaic cells (OPVCs)[33] demonstrating improved performances in terms of field-effect mobility or current density. In all these cases, NO_2-terminated SAMs were sandwiched between the organic semiconductor film and the metal contact thus generating interfaces for charge carriers injection/extraction.

NO_2-terminated SAMs have been also used to create biocompatible surfaces.[34,35] In this context, the possibility of transforming nitro groups ($-NO_2$) of the adsorbed SAM-forming molecules into primary amine functions ($-NH_2$) is particularly appealing, because they can be bioconjugated with proteins on the surface. The chemical switch from nitro to amino (e.g., $-NH_2$) group can be achieved by using several techniques: (i) electrochemistry,[36,37] (ii) exposition of the substrate to a proper reducing solution,[38,39] (iii) electron irradiation by electron-beam lithography (EBL) or extreme UV interference lithography (EUV-IL).[40−42] The last approach not only reduces the nitro group but also enables easily patterning of the SAM-coated surface.[43] As a result, a nanometer-scale array of His-tagged proteasome was successfully fabricated by selective activation and patterning of a nitro-terminated SAM achieved by EBL.[43] However, the electron beam may also induce extensive cross-linking of the aromatic SAM, jeopardizing their electron transport properties.

Here, we used 4-nitro-terphenyl-4″-methanethiol (NTM) and 4-nitro-terphenyl-3″,5″-dimethanethiol (NTD), ([1,1′;4′,1″] terphenyl-3,5-diyl)methanethiol (TM), and ([1,1′;4′,1″] terphenyl-3,5-diyl)dimethanethiol (TD) as self-assembling molecules on polycrystalline gold. Their structures display (i) one/two methanethiol groups, (ii) a terarylene conjugated backbone, and (iii) a $-NO_2$ terminal group (NTM/NTD), as shown in insets of Figure 1a,b. TM and TD have the

DOI: 10.1021/am509104z
ACS Appl. Mater. Interfaces 2015, 7, 3902−3909

same structure except for the $-NO_2$ pendant group. The methane-thiolated legs are responsible for self-assembly, whereas the conjugated backbone guarantees π-stacking interactions between molecules. These characteristics allow perpendicular arrangement of the conjugated backbones on the surface, enabling high coverage density.[30,44] The nitro group is an electro-active group (i.e., $-NO_2$), which undergoes different proton/electron equilibria,[29] that were first demonstrated for nitro-derivatives in solution,[45,46] and subsequently for molecules (self-)assembled on surfaces such as Au and glassy carbon.[47,48] As previously demonstrated,[30,49] the oligoarylene thiols used in this paper are all capable to yield well-packed SAMs on gold, even though they show different kinetics of Au passivation. All these SAMs have been implemented in OFETs, where both NTM and NTD turned out to positively dope the charge carriers density in pentacene thin-films due to the presence of the electron-withdrawing nitro group. Conversely, the presence of one or two thiol units mainly affects the kinetics of Au passivation; indeed, compounds with only one anchoring group showed faster passivation process than compounds with two thiolated legs. Computational simulations[30] highlighted how the bidentation could determine an additional constraint during the molecular packing in terms of energetics and bond lengths. In the present work, we have exploited the nitro group of NTM and NTD monolayers to reversibly modify the wettability of functionalized gold surfaces by modulating the applied potential. We first performed a deep electrochemical characterization of the monolayers assembled on gold surfaces to elucidate the mechanism of redox processes occurring at the surface, then different techniques, such as X-ray photoelectron spectroscopy (XPS), Kelvin probe (KP), and electrochemical impedance spectroscopy (EIS), have been used to get a clearer picture of these smart nanoarchitectures. Contact angle measurements allowed us to systematically study changes of the surface tension by switching from one redox state to another one (namely nitro, hydroxylamine, and nitroso groups). Finally, an array of planar Au electrodes have been fabricated in order to demonstrate the potential use of switchable SAMs for electrowetting applications.

EXPERIMENTAL SECTION

Synthesis. The synthesis of NTD, NTM, TD, and TM have been previously published.[30,49,50] The synthetic details on TM are reported in the Supporting Information.

X-ray Photoelectron Spectroscopy. XPS was performed with a double pass cylindrical mirror analyzer (PHI model 15-255G) driven at fixed pass energy of 50 eV. Mg Kα photons (1253.6 eV) were used from a VG-XR3 double anode source, operated at 15 keV and 15 mA. The spectra are here reported in binding energy, referenced to Au 4f7/2 level at 84.0 eV.

Electrochemical Measurements. Cyclic voltammetry (CV) experiments were carried out with a potentiostat/galvanostat μ-Autolab III (Metrohm, Milano, Italy) using a three-electrodes cell. A polycrystalline Au wire (outer diameter 1 mm) was used as a working electrode (WE), whereas a Pt sheet and a Ag/AgCl electrode were chosen as counter electrode (CE) and reference electrode (RE), respectively. A standardized cleaning procedure for the WE has been used as published elsewhere.[51] The WE was functionalized by simple immersion in 0.1 mM thiol solution (CH_2Cl_2 as organic solvent) at room temperature (RT) for 24 h. The electro-reduction of the SAMs have been carried out at three different pHs: (i) 1 mM H_2SO_4 (pH ~ 2), (ii) 0.1 M KCl buffered by phosphate 10 mM (pH ~ 7), and (iii) 0.1 M KCl adjusted by 10 mM KOH (pH ~ 12).

The three-electrodes cell is also exploited for EIS measurements in order to characterize the three redox states of the terminal SAM groups. In particular, all the EIS measurements have been performed in 0.1 M $NaClO_4$ and 1 mM of $[Fe(CN)_6]^{3-/4-}$. In particular, the redox potential of ferricyanide has been monitored after the electrochemical switch of the SAMs. In other terms, $-NHOH$ has been achieved by applying a linear sweep of potential spanning from +400 mV to −1.3 V. The $-NO$ group has been obtained by sweeping the potential from −1.3 V to +400 mV. For a systematic comparison, the same electrochemical switch has been performed on TM and TD SAMs.

Kelvin Probe Microscopy. Kelvin Probe measurements were performed under ambient conditions using 2 mm diameter gold tip amplifier (Ambient Kelvin Probe Package from KP Technology Ltd.). The technique provides a voltage resolution of about 5 mV. Calibration and monitoring of the probe was performed using a freshly prepared gold surface. A comprehensive description of the technique can be found in Baikie et al.[52]

Contact Angle Measurements of the Three Electro-Active Species. The Au substrates were purchased from Phasis (Geneva, Switzerland) with the following specifications: quartz glass (1 mm thick) coated by Ti as adhesive layer and an Au film (50 nm thick). The cleaning and functionalization procedures were the same applied to the WE in the electrochemical measurements.

The three different redox states of the nitro-oligoarylene thiols (NTM and NTD) have been checked by contact angle measurements (GBX model DS, from Digidrop, Bourg de Peage, France) using bidistilled water (droplets volume equal to 0.400 μL). Contact angle measurements were acquired from NTM- and NTD-coated Au for each redox state along with the crosschecks of TM and TD.

Fabrication of Au Planar Electrodes. Planar electrodes were fabricated onto the previously described Au-coated glass slides. The fabrication is carried out by laser ablation with a short-pulsed Nd:YAG infrared (IR)-laser supplied by a laser scan marker (Scriba Nanotecnologie S.r.l., Bologna, Italy). The IR-laser pulse frequency and intensity are optimized in order to find the best compromise between removal of the Au layer and roughening of the underlying quartz. A typical operation is performed at a laser driving voltage of 8.3 V, a pulse width of 10 ns, and a frequency of 15500 Hz. The laser focus is moved over the surface at a scan-rate of 2000 μm/s. Further details are already described elsewhere.[53] A computer-aided design (CAD) drawing has been prepared by using the free-software "Draftsight CAD Software" (http://www.3ds.com/products-services/draftsight-cad-software/), as shown in Supporting Information (SI) Figure S1. The electrode area is equal to 9 mm^2 and the aspect ratio (long side over short one) of the connecting grooves is equal to 290.

Electrical Merging of Droplets. The three-electrode array has been electrically measured by a homemade probe-station. The electrical voltage has been applied by means of an Agilent Source-measure unit (2 channels).

RESULTS AND DISCUSSION

Experimental evidence of the successful immobilization of the four monolayers on gold was provided by XPS investigation. Both sulfur and carbon signals were measured for bare Au and for substrates functionalized with TM, TD, NTM, and NTD (see SI Figure S2). Both the position and intensity of the corresponding peaks confirm that all the investigated molecules are assembled on gold, via a covalent S−Au bond. No traces of unbound thiols are evidenced in the spectra, and the line shape of C 1s is consistent with C in aromatic environment or C−H bonding.[54,55]

The two thiolated molecules NTM and NTD were used to functionalize polycrystalline Au substrates and were characterized by electrochemistry, KP, and contact angle measurements. Two analogous molecules, namely TM and TD, were also employed to perform countercheck experiments, since they share the same backbone as NTM and NTD, but lack the -NO_2 substituent in the terminal aromatic ring.

DOI: 10.1021/am509104z
ACS Appl. Mater. Interfaces 2015, 7, 3902−3909

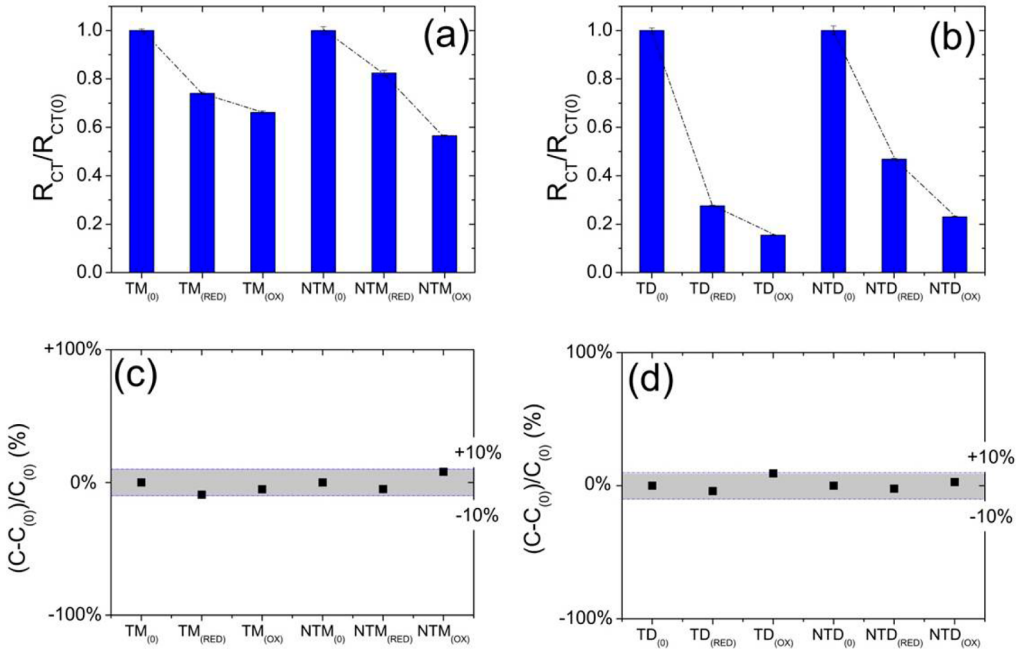

Figure 2. Normalized loss of charge transfer resistance for TM/NTM (a) and for TD/NTD (b). Relative variation of capacitance corresponding to TM/NTM (c) and TD/NTD (d).

Panels a and b of Figure 1 show the cyclic voltammograms recorded at pH = 7.0 for a polycrystalline gold electrode, functionalized with a NTM or NTD monolayer, respectively. The redox behavior of the adsorbed species is qualitatively very similar: starting from an oxidative poise, during the first voltammetric cycle (black line), a cathodic peak, with a $Ep_c \approx -0.65$ V, can be observed in the cathodic scan, and an anodic peak with $Ep_a \approx -0.08$ V is detected during the scan toward positive values. During the second voltammetric scan (red line), a new cathodic peak with $Ep_c \approx -0.10$ V appears together with its anodic counterpart, still visible at $Ep_a \approx -0.08$ V. The broad cathodic peak occurring at extremely negative potential values, which is detectable during the first scan, disappears. The electrochemical behavior observed during the second scan persists unaltered for several voltammetric cycles. Due to the similarity with electrochemical fingerprint of an analogous species (viz. nitrothiophenol SAM on Au), the signals observed for both NTM and NTD SAMs can be safely ascribed as follows: during the first voltammetric cycle, irreversible reduction of the nitro $-NO_2$ group to hydroxylamine ($-$NHOH) occurs (eq 1); from the second voltammetric scan on (eq 2), a 2-proton-2-electron reversible redox process involving the $-$NHOH/$-$NO couple is observed. While the first signal is well resolved for NTM, in the case of NTD the peak is less evident and features a sigmoidal shape.

$$R - NO_2 + 4e^- + 4H^+ \rightarrow R - NHOH + H_2O \quad (1)$$

$$R - NHOH \rightleftarrows R - NO + 2e^- + 2H^+ \quad (2)$$

where R stands for the aromatic backbone of the molecule, which is identical for NTM and NTD.

It is evident from eqs 1 and 2 that pH affects the reduction potential associated with the redox processes occurring at the surface. As a consequence, we have studied the electrochemical behavior of both NTM and NTD grafted on gold electrodes at different pH values (pH = 2, 7, 12), with a particular focus on the second, reversible step. Moving from pH = 7 to pH = 12 (see SI Figure S3), the redox potential is negatively shifted of about 0.3 V, while switching from neutral to acid values (pH = 2) conditions (SI Figure S4) leads to a comparable shift of the reduction potential E^0 in the opposite direction (see Figure 1c and SI Figure S5a). The observed pH-dependence of the redox behavior of both species is in agreement with the proposed mechanism. More precisely, the linear dependence of E^0 vs pH is 61($\pm$1)mV/pH (see SI Figure S5b) is in good agreement with the Nernstian limit.[56]

We also demonstrated that the faradaic current of the redox equilibrium ($-$NHOH/$-$NO) is due to electro-active species immobilized onto electrode surface, by studying the peak current (i_p) as a function of the scan rate (v). As shown in Figure 1d (and in SI Figure S6), the linear dependence if i_p vs v proves that this signal is not a diffusion-controlled phenomenon but the electron transfer involves adsorbed redox species.[57]

Further monitoring of the redox response of the adsorbed TM, NTM, TD, and NTD was performed by means of EIS measurements. Nyquist plots were recorded for all the adsorbed molecules (see SI Figure S7). By interpreting the data on the basis of the corresponding Randles equivalent circuit, we could obtain both the Capacitance, C, and the charge transfer resistance, R_{CT}, for all the functionalizations. The dependence of R_{CT} values on the redox state of the terminal group is displayed in Figure 2a,b. Interestingly, the main determinant to the charge transfer resistance appears to be the number of anchoring moieties rather than the presence of different nitro redox states. In fact, TM and NTM (Figure 2a) display very similar decreases of R_{CT} going from "0" (e.g., initial state) to "RED" (e.g., after a cathodic linear sweep), and then to "OX" (e.g., after an anodic linear sweep). The R_{CT} decrease is much more marked for both TD and NTD (Figure 2b), which behave much alike. This clearly shows that SAMs are perfectly assembled on Au regardless to the number of anchoring groups, but they differ once an electrical stress is provided. SAMs endowed with one anchoring group is more robust than SAMs with two anchoring groups. This

DOI: 10.1021/am509104z
ACS Appl. Mater. Interfaces 2015, 7, 3902−3909

experimental evidence is likely ascribed to the different assembly dependent to the number of anchoring group, as already described.[30]

The *C* values, reported in Figure 2c,d, suggest that no dramatic changes occur in the SAM capacitance. In fact, the slight changes of *C* values for NTD and NTM upon switching from the starting, oxidized state (0) to the reduced, hydroxylamine (RED), and back to the oxidized, nitroso (OX) are approximately as small as those displayed by both TD and TM, which lack the terminal nitro group. These findings can be justified based on the fact that neither the SAM length r_{SAM} nor its dielectric constant ϵ_{SAM} are significantly affected by the redox reactions occurring at the nitro group. The minor relative changes in *C* upon reductive and then oxidative poise also provide an indirect evidence that no significant desorption of the monolayer takes place in response to the electrical stress. It is reasonable to infer that only slight rearrangements of the SAM occur, invariably for all four investigated species.

Taken together, these EIS results indicate that two features describing the changes of electrical behavior of the functionalized surfaces, *C* and R_{CT}, following application of reductive and oxidative potentials are dominated by the "bulk" (if such an expression can be employed here) of the SAM (i.e., the whole monolayer and not just the SAM/solution interface) characterized by the nature and redox state of the terminal group.

Involving the terminal nitro group, the redox processes reflect on the shift of the contact potential of the NTM and NTD SAMs. The corresponding contact potential difference (CPD) is given by the effective molecular dipole perpendicular to the substrate, taking into account the depolarization effects due to molecular coverage.[58] Figure 3 displays relative changes

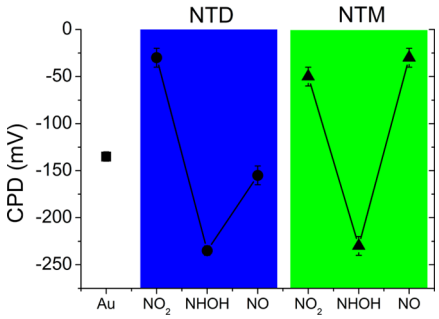

Figure 3. Contact potential difference values are shown for bare Au, NTM, and NTD. For both SAMs, the three different redox states, such as nitro (NO_2), hydroxylamine (NHOH), and nitroso (NO), have been characterized.

in the CPD upon formation of the SAM and subsequent reduction/oxidation steps. CPD values are referred to the contact potential of the probe (i.e., CP_{probe} = 0 mV).

When the SAM is formed, the CPD values for the functionalized gold undergo a shift toward more positive values for NTD and NTM, of similar magnitude for the two molecules. When the nitro group is reduced to hydroxylamine, a dramatic decrease in CPD is observed for both SAMs, as the difference between the work functions of the probe tip and the reduced functionalized surface gets as high as approximately 225 mV. Further oxidation of the terminal group to nitroso makes the CPD to raise back toward more positive values.

However, at variance with all the previous steps, where NTD closely paralleled the NTM behavior, mono- and dithiolate species diverge when the final oxidation to nitroso takes place. In fact, NTM CPD value for the nitroso state is very similar to the nitro one, suggesting a complete recovering of the initial surface potential; for the bidentate NTD, the shift upon reoxidation is much smaller. Since the terminal group is the same for both SAMs, the different behavior displayed by NTD and NTM upon the hydroxylamine-to-nitroso switch is most likely to be ascribed once again to the higher sensitivity of the dithiolate SAMs to the electrical perturbation, consistently with the aforementioned R_{CT} results. The KP investigation thus describes the combined effect of the SAM/solution interface, which dominates the changes in the contact potential upon SAM formation and reduction to hydroxylamine, and of the "bulk" of the monolayer in determining the partial or complete recovery of initial CPD values upon reoxidation to −NO.

So far, we have demonstrated the adsorption of SAM-forming molecules terminated with a nitro group onto a conductive substrate and the ability to partially reduce the $-NO_2$ termination to hydroxylamine (−NHOH), which can in turn be reversibly oxidized to −NO by controlling the applied potential. It is apparent that the different chemical nature of the terminal groups should endow the substrates with switchable properties, especially in terms of wettability toward electroactive systems.

In order to verify whether the ability to switch to different redox states, such as $-NO_2$, −NHOH, and −NO, would lead to significant changes of the surface tension of the SAM-coated Au, contact angles measurements were performed on Au functionalized with NTM or NTD before applying any potential to the electrode (therefore obtaining the contact angle, θ, for the $-NO_2$ terminated molecules) and then reversibly switching from oxidative to reducing conditions, thus acquiring θ for both the hydroxylamine and nitroso species. The corresponding values are plotted in Figure 4a. While

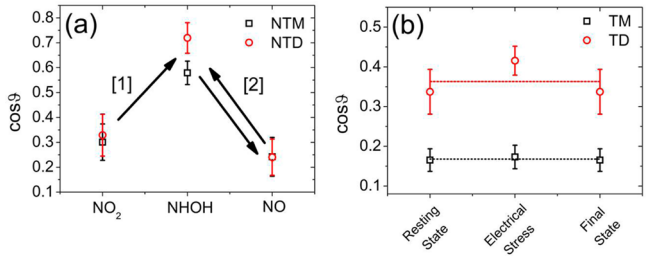

Figure 4. (a) Contact angles of water droplets relative to the three redox states for NTM (black empty squares) and NTD (red empty circles). [1] stands for the irreversible electro-reduction from NO_2 to NHOH, and [2] regards to the reversible redox reaction between NHOH and NO. All the electrochemical switches were performed at pH ∼ 12. (b) Contact angles of TM (black empty squares) and TD (red empty circles) at the same experimental conditions of NTM/NTD SAMs. The dashed lines (red and black) show the average value for both SAMs.

$-NO_2$ and −NO terminated molecules display the same degree of wettability for both SAMs, within the experimental error, a marked increase of wettability can be observed for the −NHOH exposing species.

The observed electrowetting properties are likely determined by the redox chemistry of the nitro group. As a countercheck, we have characterized two corresponding SAMs (TM and TD), lacking the nitro group, which are therefore not supposed to undergo any redox process in the same potential window. As

DOI: 10.1021/am509104z
ACS Appl. Mater. Interfaces 2015, 7, 3902−3909

expected, within the experimental error, no remarkable changes in the contact angle can be detected upon changing the substrate potential in the same range as before (see Figure 4b), thus proving the pivotal role played by the nitro group in determining the electrowetting process.

What can this electrically controlled modulation of the surface wettability be used for? SAMs with switchable properties were previously employed in two application fields such as optical lenses[9] and an electrolytic gating.[59] The observed changes in surface tension make our molecules appealing candidates for the so-termed Micro ElectroMechanical Systems (MEMs). With such an aim in mind, a real-time monitoring of the electrowetting of SAM-coated Au was first possible (see Figure S8 and Figure S9). Second, the droplet motion on a 2 planar Au electrodes under a bias of +2.4 V (data not shown) was also possible. Such a configuration enables to yield a surface tension unbalance, because the $-NO_2$ reduction takes place at the negative pole, hence the droplet motion. Along this route, we patterned an array of three planar gold electrodes by laser ablation (see Supporting Information). This Au pattern has been functionalized with NTD (see Figure 5a,b)

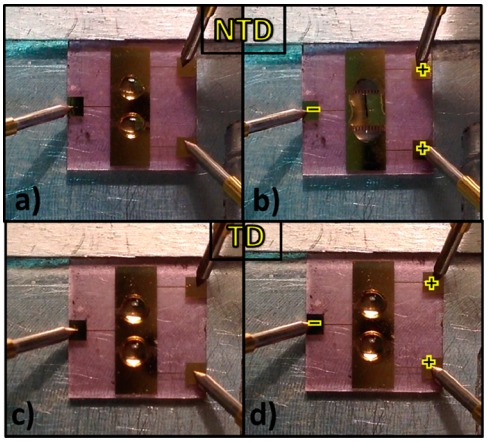

Figure 5. NTD-coated Au pattern before (a) and after (b) the electrical bias of +2.5 V. TD-coated Au pattern before (c) and after (d) the electrical bias equal to +2.5 V.

and NTM (see SI Figure S10a,b), and two water droplets (4 μL final volume) have been placed in order to guarantee an electrical connection between the two external electrodes and the central one (see Figure 5a).

Applying a potential difference of +2.5 V between the two external electrodes and the central one, the nitro terminal group is consequently reduced to hydroxylamine at the negatively charged pole, as previously mentioned. This yields a surface potential energy gradient, which drives the merging of the two droplets into a single one (see Figure 5b). The same behavior could be observed for electrodes functionalized with NTM (see SI Figure S11a,b), whereas water droplets on TD- (see Figure 5c,d) and TM-modified electrodes (see SI Figure S11c,d), used as negative controls, do not yield any electromechanical effect. Therefore, droplet motion and merging are clearly ascribed to the redox-dependent features of the NTM and NTD SAMs.

CONCLUSIONS

In summary, we have prepared and characterized gold substrates functionalized with NTM- /NTD-based SAMs and their counterchecks such as TM/TD. The presence of the terminal nitro group endows NTM and NTD with redox properties in a rather narrow potential range. Electrochemical, XPS and KP investigations elucidated the processes occurring at the surface: the $-NO_2$ group can be irreversibly reduced to $-NHOH$, which in turn can be reversibly switched into $-NO$, with robust signals that are maintained even changing the pH to acidic or basic values and/or cycling several times (see SI Figure S11). The electrically induced switching between nitro ($-NO_2$), hydroxylamine ($-NHOH$), and nitroso ($-NO$) groups leads to significant changes in the surface tension, which was exploited to demonstrate controlled electromechanical phenomena. Our results suggest that these SAMs are well-suited to be applied in low-power microelectromechanical systems paving the way toward relevant technological applications.

ASSOCIATED CONTENT

Supporting Information

(i) CAD drawing of the planar electrodes (Figure S1), (ii) the XPS spectra of sulfur and carbon atoms for the 4 SAMs (Figure S2), (iii) the electro-reduction of both NTM and NTD at pH = 12 (Figure S3) and pH = 2 (Figure S4), (iv) the electrochemical pH-dependence of NTD SAM (Figure S5), (v) the linear dependence of the peak current as a function of the scan rate for NTD (Figure S6), (vi) Nyquist plot for the 4 SAMs after voltammetric cycles (Figure S7), (vii) the electrowetting snapshots of NTM/TM (Figure S8) and NTD/TD (Figure S9) of a water droplet, (viii) the top view of the Au planar electrodes functionalized with TM and NTM SAMs (Figure S10), (ix) the overlay of 30 cyclic voltammograms corresponding to reversible redox reaction between NHOH and NO (Figure S11). Details of the chemical synthesis of TM molecule (Figure S12). This material is available free of charge via the Internet at http://pubs.acs.org/.

AUTHOR INFORMATION

Corresponding Author

*E-mail: stefano.casalini@unimore.it.

Funding

This work was funded by the European Union 7th Framework Programme [FP7/2007−2013] under Grant Agreement No. 280772, Implantable Organic Nanoelectronics (iONE-FP7) project and from Ministero dell'Istruzione, dell'Università e della Ricerca (MIUR), "Progetto PRIN 2012 prot. 2012A4Z2RY" and "Progetto PON02_00563_3316357 (PON MAAT)".

Notes

The authors declare no competing financial interest.

ACKNOWLEDGMENTS

We thank Prof. Fabio Biscarini and Dr. Tobias Cramer for the fruitful discussions.

REFERENCES

(1) Vericat, C.; Vela, M. E.; Benitez, G.; Carro, P.; Salvarezza, R. C. Self-Assembled Monolayers of Thiols and Dithiols on Gold: New Challenges for a Well-Known System. *Chem. Soc. Rev.* **2010**, *39*, 1805−1834.

(2) Calhoun, M. F.; Sanchez, J.; Olaya, D.; Gershenson, M. E.; Podzorov, V. Electronic Functionalization of the Surface of Organic Semiconductors with Self-Assembled Monolayers. *Nat. Mater.* **2008**, *7*, 84−89.

DOI: 10.1021/am509104z
ACS Appl. Mater. Interfaces 2015, 7, 3902−3909

(3) Kao, C. Y.; Lee, B.; Wielunski, L. S.; Heeney, M.; McCulloch, I.; Garfunkel, E.; Feldman, L. C.; Podzorov, V. Doping of Conjugated Polythiophenes with Alkyl Silanes. *Adv. Funct. Mater.* **2009**, *19*, 1906−1911.
(4) Kobayashi, S.; Nishikawa, T.; Takenobu, T.; Mori, S.; Shimoda, T.; Mitani, T.; Shimotani, H.; Yoshimoto, N.; Ogawa, S.; Iwasa, Y. Control of Carrier Density by Self-Assembled Monolayers in Organic Field-Effect Transistors. *Nat. Mater.* **2004**, *3*, 317−322.
(5) Ulman, A. Formation and Structure of Self-Assembled Monolayers. *Chem. Rev.* **1996**, *96*, 1533−1554.
(6) Love, J. C.; Estroff, L. A.; Kriebel, J. K.; Nuzzo, R. G.; Whitesides, G. M. Self-Assembled Monolayers of Thiolates on Metals as a Form of Nanotechnology. *Chem. Rev.* **2005**, *105*, 1103−1169.
(7) Moon, H.; Cho, S. K.; Garrell, R. L.; Kim, C.-J. Low Voltage Electrowetting-on-Dielectric. *J. Appl. Phys.* **2002**, *92*, 4080−4087.
(8) Boulas, C.; Davidovits, J.; Rondelez, F.; Vuillaume, D. Suppression of Charge Carrier Tunneling through Organic Self-Assembled Monolayers. *Phys. Rev. Lett.* **1996**, *76*, 4797−4800.
(9) Gorman, C. B.; Biebuyck, H. A.; Whitesides, G. M. Control of the Shape of Liquid Lenses on a Modified Gold Surface Using an Applied Electrical Potential across a Self-Assembled Monolayer. *Langmuir* **1995**, *11*, 2242−2246.
(10) Sondag-Huethorst, J. A. M.; Fokkink, L. G. J. Potential-Dependent Wetting of Octadecanethiol-Modified Polycrystalline Gold Electrodes. *Langmuir* **1992**, *8*, 2560−2566.
(11) Sondag-Huethorst, J. A. M.; Fokkink, L. G. J. Electrical Double Layers on Thiol-Modified Polycrystalline Gold Electrodes. *J. Electroanal. Chem.* **1994**, *367*, 49−57.
(12) Sondag-Huethorst, J. A. M.; Fokkink, L. G. J. Potential-Dependent Wetting of Electro-Active Ferrocene-Terminated Alkanethiolate Monolayers on Gold. *Langmuir* **1994**, *10*, 4380−4387.
(13) Kornyshev, A. A.; Kucernak, A. R.; Marinescu, M.; Monroe, C. W.; Sleightholme, A. E. S.; Urbakh, M. Ultra-Low-Voltage Electrowetting. *J. Phys. Chem. C* **2010**, *114*, 14885−14890.
(14) Berge, B.; Peseux, J. Variable Focal Lens Controlled by an External Voltage: An Application of Electrowetting. *Eur. Phys. J. E* **2000**, *3*, 159−163.
(15) Hayes, R. A.; Feenstra, B. J. Video-Speed Electronic Paper Based on Electrowetting. *Nature* **2003**, *425*, 383−385.
(16) Pollack, M. G.; Fair, R. B.; Shenderov, A. D. Electrowetting-Based Actuation of Liquid Droplets for Microfluidic Applications. *Appl. Phys. Lett.* **2000**, *77*, 1725−1726.
(17) Krupenkin, T.; Taylor, J. A. Reverse Electrowetting as a New Approach to High-Power Energy Harvesting. *Nat. Commun.* **2011**, *2*, 1−7.
(18) Jun Lee, S.; Lee, S.; Hyoung Kang, K. Droplet Jumping by Electrowetting and Its Application to the Three-Dimensional Digital Microfluidics. *Appl. Phys. Lett.* **2012**, *100*, 081604.
(19) Galletto, P.; Girault, H. H.; Gomis-Bas, C.; Schiffrin, D. J.; Antoine, R.; Broyer, M.; Brevet, P. F. Second Harmonic Generation Response by Gold Nanoparticles at the Polarized Water/2-Octanone Interface: from Dispersed to Aggregated Particles. *J. Phys.: Condens. Matter* **2007**, *19*, 375108.
(20) Su, B.; Fermín, D. J.; Abid, J.-P.; Eugster, N.; Girault, H. H. Adsorption and Photoreactivity of CdSe Nanoparticles at liquid|Liquid Interfaces. *J. Electroanal. Chem.* **2005**, *583*, 241−247.
(21) Chinwangso, P.; Jamison, A. C.; Lee, T. R. Multidentate Adsorbates for Self-Assembled Monolayers. *Acc. Chem. Res.* **2011**, *44*, 511−519.
(22) Salomon, A.; Cahen, D.; Lindsay, S.; Tomfohr, J.; Engelkes, V. B.; Frisbie, C. D. Comparison of Electronic Transport Measurements on Organic Molecules. *Adv. Mater.* **2003**, *15*, 1881−1890.
(23) Casalini, S.; Shehu, A.; Destri, S.; Porzio, W.; Pasini, M. C.; Vignali, F.; Borgatti, F.; Albonetti, C.; Leonardi, F.; Biscarini, F. Organic Field-Effect Transistors as New Paradigm for Large Area Molecular Junctions. *Org. Electron.* **2012**, *13*, 789−795.
(24) Casalini, S.; Shehu, A.; Leonardi, F.; Albonetti, C.; Borgatti, F.; Biscarini, F. Hydrophilic Self-Assembly Monolayers for Pentacene-Based Thin-Film Transistors. *Org. Electron.* **2013**, *14*, 1891−1897.
(25) Chidsey, C. E. D.; Loiacono, D. N. Chemical Functionality in Self-Assembled Monolayers: Structural and Electrochemical Properties. *Langmuir* **1990**, *1*, 682−691.
(26) Esplandiù, M. J.; Hagenstro, H.; Kolb, D. M. Functionalized Self-Assembled Alkanethiol Monolayers on Au(111) Electrodes: 1. Surface Structures and Electrochemistry. *Langmuir* **2001**, *17*, 828−838.
(27) Morgenthaler, S. M.; Lee, S.; Spencer, N. D. Submicrometer Structure of Surface-Chemical Gradients Prepared by a Two-Step Immersion Method. *Langmuir* **2006**, *22*, 2706−2711.
(28) Ballav, N.; Shaporenko, A.; Terfort, A.; Zharnikov, M. A Flexible Approach to the Fabrication of Chemical Gradients. *Adv. Mater.* **2007**, *19*, 998−1000.
(29) Lund, H.; Hammerich, O. *Organic Electrochemistry*; Marcel Dekker: New York, 2001.
(30) Casalini, S.; Berto, M.; Leonardi, F.; Operamolla, A.; Bortolotti, C. A.; Borsari, M.; Sun, W.; Di Felice, R.; Corni, S.; Albonetti, C.; Hassan Omar, O.; Farinola, G. M.; Biscarini, F. Self-Assembly of Mono- and Bidentate Oligoarylene Thiols onto Polycrystalline Gold. *Langmuir* **2013**, *29*, 13198−131208.
(31) Gundlach, D. J.; Jia, L.; Jackson, T. N. Pentacene TFT with Improved Linear Region Characteristics Using Chemically Modified Source and Drain Electrodes. *IEEE Electron Device Lett.* **2001**, *22*, 571−573.
(32) Kim, D. H.; Chung, C. M.; Park, J. W.; Oh, S. Y. Effect of ITO Surface Modification Using Self-Assembly Molecules on the Characteristics of OLEDs. *Ultramicroscopy* **2008**, *108*, 1233−1236.
(33) Bedis, H. Effect of Self-Assembled Monolayers on the Performance of Organic Photovoltaic Cells. *J. Surf. Eng. Mater. Adv. Technol.* **2011**, *01*, 42−50.
(34) Amin, I.; Steenackers, M.; Zhang, N.; Beyer, A.; Zhang, X.; Pirzer, T.; Hugel, T.; Jordan, R.; Gölzhäuser, A. Polymer Carpets. *Small* **2010**, *6*, 1623−1630.
(35) Zheng, Z.; Nottbohm, C. T.; Turchanin, A.; Muzik, H.; Beyer, A.; Heilemann, M.; Sauer, M.; Gölzhäuser, A. Janus Nanomembranes: A Generic Platform for Chemistry in Two Dimensions. *Angew. Chem., Int. Ed. Engl.* **2010**, *49*, 8493−8497.
(36) Tsutsumi, H.; Furumoto, S.; Morita, M.; Matsuda, Y. Electrochemical Behavior of a 4-Nitrothiophenol Modified Electrode Prepared by the Self-Assembly Method. *J. Colloid Interface Sci.* **1995**, *171*, 505−511.
(37) Nielsen, J. U.; Esplandiu, M. J.; Kolb, D. M. 4-Nitrothiophenol SAM on Au(111) Investigated by In Situ STM, Electrochemistry and XPS. *Langmuir* **2001**, *17*, 3454−3459.
(38) Al-Rawashdeh, N. A. F.; Azzam, W.; Wöll, C. Fabrication of an Amino-Terminated Organic Surface by Chemical Conversion of a Nitro-Terminated Self-Assembled Monolayer. *Z. Phys. Chem.* **2008**, *222*, 965−978.
(39) Eck, B. W.; Stadler, V.; Geyer, W.; Zharnikov, M.; Gölzhäuser, A.; Grunze, M. Generation of Surface Amino Groups on Aromatic Self-Assembled Monolayers by Low Energy Electron Beam: A First Step towards Chemical Lithography. *Adv. Mater.* **2000**, *12*, 805−808.
(40) Gölzhäuser, A.; Eck, W.; Geyer, W.; Stadler, V.; Weimann, T.; Hinze, P.; Grunze, M. Chemical Nanolithography with Electron Beams. *Adv. Mater.* **2001**, *13*, 806−809.
(41) Gölzhäuser, A.; Geyer, W.; Stadler, V.; Eck, W.; Grunze, M.; Edinger, K.; Weimann, T.; Hinze, P. Nanoscale Patterning of Self-Assembled Monolayers with Electrons. *J. Vac. Sci. Technol., B: Microelectron. Nanometer Struct.–Process., Meas., Phenom.* **2000**, *18*, 3414−3418.
(42) Schmelmer, U.; Jordan, R.; Geyer, W.; Eck, W.; Gilzh, A.; Grunze, M.; Ulman, A. Surface-Initiated Polymerization on Self-Assembled Monolayers: Amplification of Patterns on the Micrometer and Nanometer Scale. *Angew. Chem., Int. Ed. Engl.* **2003**, *42*, 559−563.
(43) Turchanin, A.; Tinazli, A.; El-Desawy, M.; Großmann, H.; Schnietz, M.; Solak, H. H.; Tampé, R.; Gölzhäuser, A. Molecular Self-Assembly, Chemically Lithography, and Biochemical Tweezers: A Path for the Fabrication of Functional Nanometer-Scale Protein Arrays. *Adv. Mater.* **2008**, *20*, 471−477.

DOI: 10.1021/am509104z
ACS Appl. Mater. Interfaces 2015, 7, 3902−3909

(44) Bruno, G.; Babudri, F.; Operamolla, A.; Bianco, G. V.; Losurdo, M.; Giangregorio, M. M.; Hassan Omar, O.; Mavelli, F.; Farinola, G. M.; Capezzuto, P.; Naso, F. Tailoring Density and Optical and Thermal Behavior of Gold Surfaces and Nanoparticles Exploiting Aromatic Dithiols. *Langmuir* **2010**, *26*, 8430−8440.
(45) Rubinstein, I. Voltammetric Study of Nitrobenzene and Related Compounds on Solid Electrodesin Aqueous Solution. *J. Electroanal. Chem.* **1985**, *183*, 379−386.
(46) Nishihara, C.; Shindo, H. Two Distinct Surface Conditions of a Gold Electrode from the Viewpoint of the Reduction of Nitrobenzene in Aqueous Alkaline Solution. *J. Electroanal. Chem.* **1987**, *221*, 245−250.
(47) Ortiz, B.; Saby, C.; Champagne, G. Y.; Bélanger, D. Electrochemical Modification of a Carbon Electrode Using Aromatic Diazonium Salts. 2. Electrochemistry of 4-Nitrophenyl Modified Glassy Carbon Electrodes in Aqueous Solution. *J. Electroanal. Chem.* **1998**, *455*, 75−81.
(48) Vase, K. H.; Holm, A. H.; Pedersen, S. U.; Daasbjerg, K. Immobilization of Aryl and Alkynyl Groups onto Glassy Carbon Surfaces by Electrochemical Reduction of Iodonium Salts. *Langmuir* **2005**, *21*, 8085−8089.
(49) Casalini, S.; Leonardi, F.; Bortolotti, C. A.; Operamolla, A.; Hassan Omar, O.; Paltrinieri, L.; Albonetti, C.; Farinola, G. M.; Biscarini, F. Mono/Bidentate Thiol Oligoarylene-Based Self-Assembled Monolayers (SAMs) for Interface Engineering. *J. Mater. Chem.* **2012**, *22*, 12155−121633.
(50) Operamolla, A.; Hassan Omar, O.; Babudri, F.; Farinola, G. M.; Naso, F.; Chimica, D.; Uni, V.; Chimica, C. N. R. I.; Orabona, V. Synthesis of S-Acetyl Oligoarylenedithiols via Suzuki−Miyamura Cross-Coupling. *J. Org. Chem.* **2007**, *72*, 10272−10275.
(51) Casalini, S.; Battistuzzi, G.; Borsari, M.; Ranieri, A.; Sola, M. Catalytic Reduction of Dioxygen and Nitrite Ion at a Met80Ala Cytohrome c-Functionalized Electrode. *J. Am. Chem. Soc.* **2008**, *130*, 15099−150104.
(52) Baikie, I. D.; Mackenzie, S.; Estrup, P. J. Z.; Meyer, J. A. Noise and the Kelvin Method. *Rev. Sci. Instrum.* **1991**, *62*, 1326−1332.
(53) Campana, A.; Cramer, T.; Greco, P.; Foschi, G.; Murgia, M.; Biscarini, F. Facile Maskless Fabrication of Organic Field-Effect Transistors on Biodegradable Substrates. *Appl. Phys. Lett.* **2013**, *103*, 073302.
(54) Duwez, A. Exploiting Electron Spectroscopies to Probe the the Structure and Organization of Self-Assembled Monolayers: A Review. *J. Electron Spectrosc. Relat. Phenom.* **2004**, *134*, 97−138.
(55) Shaporenko, A.; Terfort, A.; Grunze, M.; Zharnikov, M. A Detailed Analysis of the Photoemission Spectra of Basic Thioaromatic Monolayers on Noble Metal Substrates. *J. Electron Spectrosc. Relat. Phenom.* **2006**, *151*, 45−51.
(56) Bergveld, I. P. ISFET, Theory and Practice In. *IEEE Sensor Conference Toronto* **2003**, 1−26.
(57) Bard, A. J.; Faulkner, L. R. *Electrochemical Methods: Fundamentals and Applications*; John Wiley & Sons, Inc.: New York, 2001.
(58) Liscio, A.; Palermo, V.; Paolo, S. Nanoscale Quantitative Measurements of the Potential of Charged Nanostructures by Electrostatic and Kelvin Probe Microscopy: Unraveling Electronic Processes in Complex Materials. *Acc. Chem. Res.* **2010**, *43*, 541−550.
(59) Abbott, N. L.; Whitesides, G. M. Potential-Dependent Wetting of Aqueous Solutions on Self-Assembled Monolayers Formed from 15-(Ferrocenylcarbonyl)Pentadecanethiol on Gold. *Langmuir* **1994**, *10*, 1493−1497.

DOI: 10.1021/am509104z
ACS Appl. Mater. Interfaces 2015, 7, 3902−3909